AN ROI-BASED MEDICAL IMAGE HIDING METHOD

PEI-YAN PAI[1], CHIN-CHEN CHANG[1,2], YUNG-KUAN CHAN[3] AND CHIA-MING LIU[2]

[1]Department of Computer Science
National Tsing Hua University
No. 101, Section 2, Kuang-Fu Rd., Hsinchu 300, Taiwan
d938338@oz.nthu.edu.tw

[2]Department of Information Engineering and Computer Science
Feng Chia University
No. 100, Wenhwa Rd., Seatwen, Taichung 407, Taiwan
ccc@cs.ccu.edu.tw; sam30525sam@gmail.com

[3]Department of Management Information Systems
National Chung Hsing University
No. 250, Kuokuang Rd., Taichung 402, Taiwan
ykchan@nchu.edu.tw

ABSTRACT. *Transmitting medical images among health care professionals, providers, and organizations via the Internet has become popular. However, illegal attackers or hackers can easily grab, duplicate, or revise the medical images on the Internet. Generally, a medical image should be kept intact for accurately diagnosing the patient's condition. A reversible image hiding method can restore the original medical image losslessly only from the stego-image. The reversible image hiding method can be used to conceal secret data in a medical image; however, it can only carry a few secret data. On the contrary, an irreversible image hiding method can generally hold much more secret data. In a medical image, "region of interest" (ROI) is a region which contains important information and must be stored without any distortion. This paper hence proposes an ROI-based image hiding method which embeds secret data in non-ROI by an irreversible image hiding method and in ROIs by a reversible image hiding method. The experimental results indicate that the proposed method can not only provide a good performance in data embedding capacity and stego-image quality but can also restore the ROIs without any distortion.*

Keywords: Irreversible image hiding, Reversible image hiding, ROI, Medical image, Image segmentation

1. **Introduction.** In recent years, most medical information has been digitized [5]. It is often necessary to transmit medical information among patients, medical professionals, health care providers, and health care organizations, and it is very fast and convenient to transmit digitized medical information via the Internet. However, the illegal attackers or hackers can easily get the information through the Internet and then duplicate or revise it. Image hiding is one of feasible methodologies for protecting the important information from being stolen. In telemedicine applications, patient's medical records are linked to the medical secrecy. Therefore, confidentiality of patient's data can be achieved by hiding "electronic patient's report" (EPR) data in related medical images. For a successful medical image hiding method, after embedding secret data in a medical image, the original medical image can be recovered from the stego-image without any distortion since a medical image is often responsible for accurate diagnosis.

In image hiding, an image, called a cover image, is selected to embed secret data. After the secret data are embedded, the cover image is transformed into a stego-image. When embedding secret data in a cover image, an irreversible image hiding method will cause noticeable distortion in the corresponding stego-image [1,3,4,9]; however, the illegal attacker cannot directly detect the difference between the cover image and stego-image through human eyes. Recently, some reversible image hiding theories and methods [2,6,9] have been developed. However, the reversible image hiding methods generally provide very low data embedding rate. In this paper, an ROI-based hiding method is hence proposed.

A medical image is often responsible for accurate diagnosis; hence, the quality of a medical image is very important for accurate diagnosis. In a medical image, "region of interest" (ROI) is a region which contains important information and must be stored without any distortion [11], i.e., the cytoplast in the cervical smear image, shown in Figure 1(b). Generally, ROI can be defined by a doctor manually according to different particular applications. For example, Figures 1(a) and 1(c) show a cervical smear image and a brain "magnetic resonance imaging" (MRI) image. The white rectangles in Figures 1(b) and 1(d) indicate the ROIs.

(a) Cervical smear image   (b) ROI of Figure 1(a)

(c) Brain MRI image   (d) ROI of Figure 1(c)
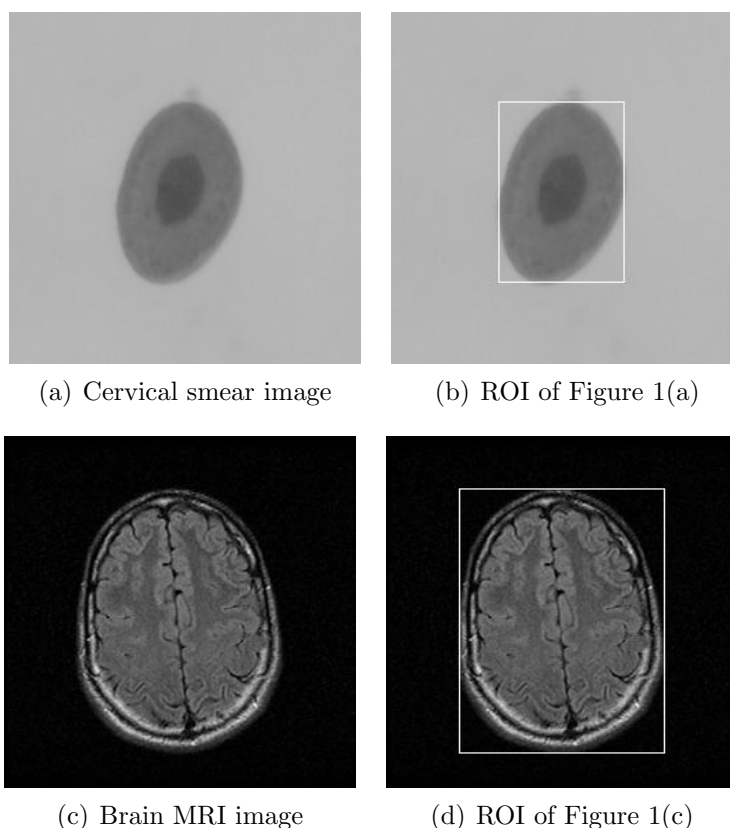
FIGURE 1. Examples of ROIs in two medical images

An irreversible image hiding method can provide a high data embedding rate but it will destroy the cover image. In a reversible image hiding method, the cover image can be reconstructed without any distortion; however, a very low data embedding rate is obtained. The proposed ROI-based image hiding method will cut off the ROIs from a cover medical image, and then conceal secret data in ROIs by a reversible image hiding

method and in non-ROI by an irreversible image hiding method. In the proposed ROI-based image hiding method, not only the ROIs can be recovered losslessly, but also a high data embedding rate is obtained.

2. **ROI-Based Image Hiding Method.** The ROI-based image hiding method consists of three stages: ROI segmentation, non-ROI hiding and ROI hiding. The ROI segmentation stage is to separate the ROIs from the cover image, the non-ROI hiding stage to bury the secret data in non-ROI by an irreversible image hiding method, and the ROI hiding stage to hide the secret data in ROIs by a reversible image hiding method. This section will describe these three stages in detail.

2.1. **ROI segmentation stage.** Image segmentation plays an important role in computer vision and image processing. The aim of image segmentation is to extract the interested objects from an image. Otsu's thresholding method [7] is one of widely-used thresholding methods in image segmentation due to its simple, effective and easy implementation. Otsu's thresholding method decides the optimal threshold by maximizing the between-class variances or minimizing the within-class variances of the data in the categorized classes.

Nevertheless, Otsu's thresholding method often gives imprecise thresholds when the variances or quantities of data among classes are quite different. Pai et al. [8] proposed an "adaptive threshold detector" (ATD), which considers the standard deviations, quantities, and group intervals of the data in all classified classess as the factors deciding the optimal thresholds. ATD can overcome the drawback of Otsu's thresholding method. Generally, the interested objects and background on a medical image can be distinguished by their gray-level intensities so that the thresholding method can be applied to separating the interested objects and background. Hence, in the ROI-based image hiding method, ATD is employed to select the most suitable threshold for separating the interested objects from the medical image.

Let x_{Min} and x_{Max} be the minimal and maximal gray-level intensities in a medical image, the pixels in which will be divided into two classes C_1 and C_2 where the gray-level intensities of the pixels in C_1 are in $\{x_{Min}, x_{Min+1}, \ldots, t\}$ and those in C_2 are in $\{t+1, t+2, \ldots, x_{Max}\}$ by repeatedly given threshold $t = \{x_{Min+1}, x_{Min+2}, \ldots, x_{Max-1}\}$. Also let $x_{g,i}$ be the ith gray-level intensity in C_g and $n_{g,i}$ be the number of pixels with the ith gray-level intensity in C_g. The group interval $R_g(t)$ of C_g is defined as:

$$R_g(t) = \begin{cases} t - x_{Min}, & \text{if } g = 1, \\ x_{Max} - t, & \text{otherwise.} \end{cases} \tag{1}$$

The percentage $P_g(t)$ of the data quantity in the gth group to the entire data set is:

$$p_g(t) = \frac{\displaystyle\sum_{i=1}^{R_2(t)} n_{g,i}}{\displaystyle\sum_{g=1}^{2} \sum_{i=1}^{R_2(t)} n_{g,i}}. \tag{2}$$

The average data value M_g of the gth group is:

$$M_g = \frac{\sum_{i=1}^{R_2(t)} n_{g,i} \times x_{g,i}}{\sum_{i=1}^{R_2(t)} n_{g,i}}. \tag{3}$$

The standard deviation $Std_g(t)$ of the data values in the gth group is:

$$Std_g(t) = \sqrt{\frac{\sum_{i=1}^{R_g(t)} \sum^{n_{g,j}} (x_{g,j} - M_g)^2}{\sum_{i=1}^{R_2(t)} n_{g,i}}}. \tag{4}$$

ATD computes the optimal thresholds T^* by the following formula:

$$T^* = Arg\left(\min_t \left(\sum_{g=1}^{2} \frac{P_g(t)Std_g(t)^{r_1}}{R_g(t)^{r_2}}\right)\right), \tag{5}$$

where r_1 and r_2 are two given parameters that describe the relationships between R_g, P_g and Std_g. The most appropriate r_1 and r_2 can be decided by a genetic algorithm [9] via the accumulated historical data.

Figure 2 shows the medical images and their gray-level histograms. The two highest peaks in the histogram describe the gray-level distributions of background and interested object, respectively. The gray-level distributions of the interested object and background on a medical image can be separated by a threshold derived from the gray-level histogram of the image. The ROI-based image hiding method uses ATD to separate the interested object and background of the medical image.

Let I be a medical image, $I(x, y)$ be a pixel located at the coordinates (x, y) on I, and the optimal threshold T^* be computed from the gray-level histogram of I by ATD. Then, a binary image I_b is generated by:

$$I_b(x, y) = \begin{cases} 0, & \text{if } I(x, y) \geq T^*, \\ 1, & \text{otherwise,} \end{cases} \tag{6}$$

where I_b is a binary image and a **1**-bit (resp. **0**-bit) denotes a black pixel (resp. a white pixel). We name $I(x, y)$ an interested pixel only if $I_b(x, y) = 0$, where all the adjacent interested pixels comprise an interested region. In this paper, we call the minimal rectangle, enclosing the interested region, an ROI, and after cutting off the ROIs from I the remaining of I is called non-ROI. Figures 3(a) and 3(b) display the I_b and the detected ROI of the image in Figure 2(a).

2.2. **Non-ROI hiding stage.** The "least significant bit" (LSB) replacement method [1], where the k-LSBs of one pixel in a cover image are replaced with k-bits of secret data, is one of commonly used irreversible image hiding methods. Chan et al. [1] proposed a "simple LSB substitution" (SLSB) method which provides a high quality of stego-image with low computational complexity and supplies a high embedding capacity. Therefore, the ROI-based image hiding method applies the SLSB method [1] to embeding secret data in non-ROI.

(a) Cervical smear image

(b) The histogram of Figure 2

(c) Brain MRI image

(d) The histogram of Figure 2
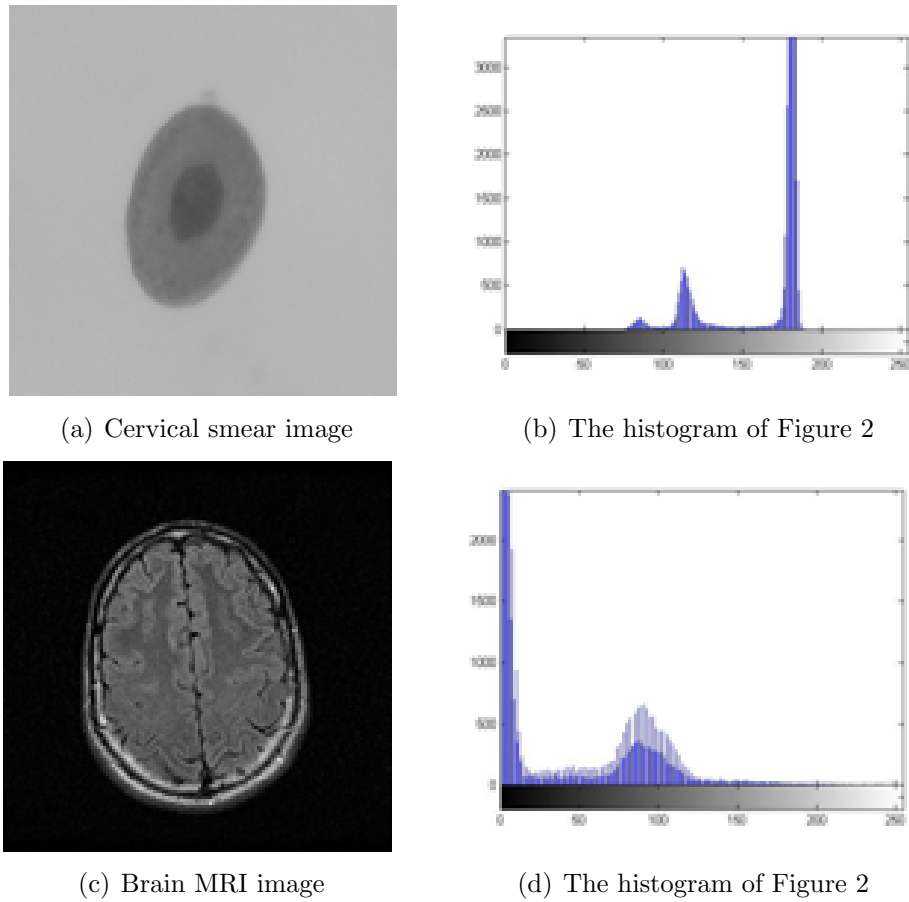
FIGURE 2. The medical images and their gray-level histograms

(a) I_b

(b) ROI
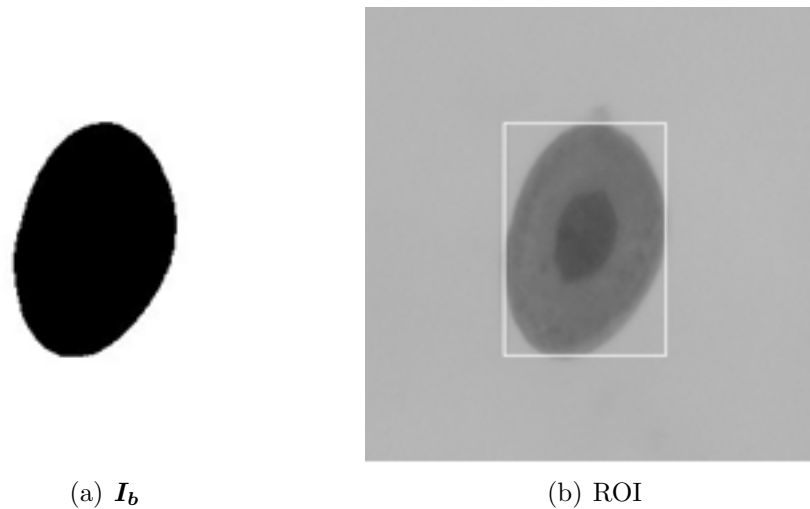
FIGURE 3. The I_b and ROI of the image in Figure 2(a)

An ROI R can be described by the most left-up and the most right-down coordinates of R. Assume that SD is the secret data which will be concealed in I and there are n_r ROIs in I which are respectively indicated by $\{(x_{11}, y_{11}), (x_{12}, y_{12})\}$, $\{(x_{21}, y_{21}), (x_{22}, y_{22})\}$, $\ldots$, $\{(x_{n_r1}, y_{n_r1}), (x_{n_r2}, y_{n_r2})\}$, where (x_{i1}, y_{i1}) are the most left-up coordinates and (x_{i2}, y_{i2}) are the most right-down coordinates of the ith ROI. First, the integers n_r, x_{11},

$y_{11}, x_{12}, y_{12}, x_{21}, y_{21}, x_{22}, y_{22}, \ldots, x_{n_r1}, x_{y_r1}, x_{n_r2}, y_{n_r2}$ and $|SD|$ are converted into binary digits and then are concatenated into the front of SD to become a binary string SD, where $|SD|$ is the number of bits in SD.

After that, to prevent an illegal attacker from figuring out the messages in SD', the ROI-based image hiding method takes a private key PK as the seed of a random number generator G to generate a binary string K, where $|K| = |SD'|$. Then, the system computes $SD'' = K \oplus SD'$, where $\oplus$ is the EXCLUSIVE OR operator.

If $|SD''|k \times n_{NROI}$, the ROI-based image hiding method sets SD''_{NROI} to SD'' and SD''_{Rem} to an empty string; otherwise, it gives the left most $k \times n_{NROI}$ bits of SD'' to SD''_{NROI} and the remainder of SD'' to SD''_{Rem}. Here, n_{NROI} is the number of pixels in non-ROI and the SLSB method will replace the $k - LSBs$ of a pixel in non-ROI by k-bits of secret data. Then, the ROI-based image hiding method will embed SD''_{NROI} in non-ROI and SD''_{Rem} in ROIs.

Beginning at the most left-up pixels of non-ROI, the ROI-based image hiding method buries each pixel on SD''_{NROI} in non-ROI from left to right and up to down pixel by pixel. Let $I(x, y)$ be the gray-level intensity of the ith pixel in non-ROI that is located at the coordinates (x, y) of I, S_i be the ith substring of that will be embedded in the ith pixel of non-ROI, and $k(= |S_i|)$ be the number of least significant bits of $I(x, y)$ that will be replaced by S_i and $S_i\{0, 1, \ldots, 2^k - 1\}$. The SLSB method computes the embedding error $\delta(x, y)$ between $I(x, y)$ and the stego-image I' by:

$$\delta(x, y) = \left(I(x, y) \bmod 2^k\right) - S_i. \tag{7}$$

Then $I'(x, y)$ can be calculated as follows:

$$I'(x, y) = \begin{cases} I(x, y) - (\delta(x, y) + 2^k), & \text{if } -2^k < \delta(x, y) < -2^{k-1} \text{ and } I(x, y) \geq 2^k, \\ I(x, y) - (\delta(x, y) - 2^k), & \text{if } 2^{k-1} < \delta(x, y) < 2^k \text{ and } I(x, y) \geq 255 - 2^k, \\ I(x, y) - \delta(x, y), & \text{otherwise.} \end{cases} \tag{8}$$

3. **ROI Hiding Stage.** Many reversible image hiding methods have been proposed [2,5,6,9]; however, these reversible image hiding methods provide a limited data embedding rate. Chang et al. [2] proposed a high payload frequency-based reversible image hiding (HPFRIH) method, in which a cover image was first transformed from the spatial domain into HDWT-based frequency domain. Then, secret data was embedded in the coefficients on high-frequency bands of the frequency domain cover image. This method adopts an adaptive arithmetic coding method to compress the high-frequency coefficients and embeds the compressed data in the high-frequency coefficients, so that the cover image can be restored with lossless. Without transmitting extra data to the receiver, the HPFRIH method is simple and affords not only a high embedding capacity but also a good stego-image quality. The ROI-based image hiding method hence employs the HPFRIH method to hide SD''_{Rem} in ROIs of I' only if $|SD''_{Rem}| > 0$.

Let (x_{i1}, y_{i1}) and (x_{i2}, y_{i2}) be the most left-up and the most right-down coordinates of the ith ROI in I'. To solve the underflow/overflow problem, for the ith ROI, the HPFRIH method firstly transforms I' into by the following program segment:
where BM is an $(x_{i2} - x_{i1}) \times (y_{i2} - y_{i1})$ bit-map array which is adopted to record the locations of the pixels with intensities less than $2^{k'}$ or greater than $255 - 2^{k'}$ and k' is the number of embedded secret bits embedded into a coefficient of the high-frequency band.

Next, "Haar discrete wavelet transform" (HDWT) function is implemented by using horizontal operation and vertical operation. First, the horizontal operation is used to decompose the ith ROI on I'' into a low-frequency band L and a high-frequency band H. After that, the vertical operation, is respectively used to partition L and H into LL,

$$
\begin{aligned}
&I'' = I' \\
&\text{For } x = x_{i1} \text{ to } x_{i2} \\
&\quad \text{For } y = y_{i1} \text{ to } y_{i2} \\
&\qquad \text{If } (I'(x,y) < 2^{k'}) \text{ then} \\
&\qquad\quad (x,y) = I''(x,y) + 2^{k'} \text{ and } BM[x - x_{i1}, y - y_{i2}] = 1 \\
&\qquad \text{Else if } (I'(x,y) > 255 - 2^{k'}) \text{ then} \\
&\qquad\quad (x,y) = I''(x,y) - 2^{k'} \text{ and } BM[x - x_{i1}, y - y_{i2}] = 1 \\
&\qquad \text{Else} \\
&\qquad\quad (x,y) = I''(x,y) \text{ and } BM[x - x_{i1}, y - y_{i2}] = 0
\end{aligned}
$$

LH, HL, and HH frequency bands, each of which is 1/4 of the original image size. HH is the high-frequency band, LL is the low-frequency band, and LH and HL are two middle-frequency bands.

Then, the HH is decomposed into three matrices, each with the same size as HH: (1) sign matrix HHS, (2) integer matrix HHI, and (3) decimal matrix HHD. The positive and negative signs of coefficients in HH are represented by 0 and 1 in HHS, respectively. The k' least significant bits of all the coefficients in HHI are copied to an $\left(\dfrac{x_{i2} - x_{i1}}{2}\right) \times \left(\dfrac{y_{i2} - x_{i1}}{2}\right)$ array ED. After that, ED and BM are concatenated into a binary string ED', and ED' are encoded by the adaptive arithmetic coding method, where the compressed codes of ED' is defined as CD. Finally, the HPFRIH method concatenates SD''_{Rem}, $|CD|$ and CD together into a binary string HD and embeds HD into the coefficients in HHI by using the LSB replacement method. The hiding process is:

$$
\begin{aligned}
&\text{For } x = 1 \text{ to } \frac{x_{i2} - x_{i1}}{2} \\
&\quad \text{For } y = 1 \text{ to } \frac{y_{i2} - y_{i1}}{2} \\
&\qquad \text{Remove the leftmost } k' \text{ bits } u \text{ from } HD \\
&\qquad \text{Replace the } k' \text{ least significant bits of } HHI[x,y] \text{ with } u
\end{aligned}
$$

HHS, HHI and HHD are then combined into HH' by:

$$
\begin{aligned}
&\text{For } x = 1 \text{ to } \frac{x_{i2} - x_{i1}}{2} \\
&\quad \text{For } y = 1 \text{ to } \frac{y_{i2} - y_{i1}}{2} \\
&\qquad HH'[x,y] = HHI[x,y] + HHD[x,y] \\
&\qquad \text{If } HHS[x,y] = 1, \text{ then } HH'[x,y] = -1 \times HH[x,y]
\end{aligned}
$$

Finally, LL, LH, HL and HH' are converted into a spatial domain format by invert-HDWT. Let I_s be the stego image after hiding SD''_{NROI} in non-ROI and SD''_{Rem} in ROIs of I.

4. **Secret Data Extracting.** This section is to draw out the embedded secret data SD from I_s. Beginning at the most left-up pixel LU of non-ROI, the ROI-based image hiding method visits each pixel in non-ROI on I_s following the same visiting order in

the ROI hiding stage. When visiting each pixel $I_s(x, y)$, the ROI-based image hiding method computes $S' = I_s(x, y) \bmod 2^k$, uses the same private key PK as the seed of the random number generator G to generate a k-bit binary string B, and then creates $S = B \oplus S$. Besides that, the ROI-based image hiding method first extracts an integer n_r from the first $\frac{n_i}{k}$ pixels of non-ROI. Assume that each integer indicated by n_i bits. n_r describes the number of ROIs in I_s. Next, the ROI-based image hiding method extracts the integers x_{11}, y_{11}, x_{12}, y_{12}, x_{21}, y_{21}, x_{22}, y_{22}, ..., x_{n_r1}, y_{n_r1}, x_{n_rx}, y_{n_r2}, $|SD|$ from the non-ROI in I_s. It then puts out SD''_{NROI} from the next $\frac{SD''_{NROI}}{k}$ pixels on the non-ROI.

According to n_r, x_{11}, y_{11}, x_{12}, y_{12}, x_{21}, y_{21}, x_{22}, y_{22}, ..., x_{n_r1}, y_{n_r1}, x_{n_rx}, y_{n_r2} then the ROI-based image hiding method can extract from the ROIs on I_s. The ROI-based image hiding method first transforms I_s into a frequency domain image by one-level HDWT decomposition, computes $|SD''_{Rem}| = |SD| - |SD''_{NROI}|$, and extracts SD''_{Rem} with $|SD''_{Rem}|$ bits from the $k' - LSBs$ of HHI in HH. Then, a binary string BS with $|SD''_{Rem}|$ bits is created by G and $BS' = BS \oplus |SD''_{Rem}|$ is computed. BS' is the secret data embedded in ROIs. Next, the ROI-based image pulls out an integer $|CD|$ and the binary string CD with $|CD|$ bits from the LSBs of the remaining HHI in HH. The adaptive arithmetic coding method is then adopted to reconstruct ED' via CD, where the first $\dfrac{k'}{k' + 1}$ bits of ED' are ED and the last $\dfrac{1}{k' + 1} \times |ED'|$ bits of ED' are BM. The k'-LSBs of all the coefficients in HHI are replaced by ED. Afterwards, HHS, HHI and HHD are combined into HH' and the LL, LH, HL and HH' are invert-HDWT into the spatial domain image I''. Next, for each pixel P with gray-level intensity g in ROIs.

> If (P corresponds to a 1-bit in BM) and ($g < 2 \times 2^{k'}$) then $g = g - 2^{k'}$
>   Else If (P corresponds to a 1-bit in BM) and ($255 - 2 \times 2^{k'} < g \leq 255$) then $g = g + 2^{k'}$

Finally, I'' is changed into I', the ROIs of which are completely the same as the ROIs in I.

5. **The Experimental Results and Analysis.** This section is to investigate the performance of the ROI-based image hiding method and to compare the performance with those of other image hiding methods, including HPFBRIH [2], Ni et al.'s [6], Tian's [10] and SLSB methods [1], by experiments. In these experiments, twelve 256×256 gray-level medical images, consisting of six cervical smear images and six brain MRI images shown in Figure 4, will be used as test images. Peak signal-to-noise ratio ($PSNR$) is adopted to measure the visual image quality between the cover image I and the stego-image I_s. Let H and W be the height and width of I and I_s, respectively. $PSNR$ is defined as:

$$PNSR = 10 \log_2 \left(\frac{255^2}{MSE} \right) (dB), \quad MSE = \frac{1}{H \times W} \sum_{x=1}^{H} \sum_{y=1}^{W} (I(x, y) - I_s(x, y))^2. \quad (9)$$

Data embedding rate is used to estimate the embedding capacity of an image hiding method. Here, data embedding rate R is computed by

$$R = \frac{\text{the size of secret data}}{H \times W} (\text{bit per pixel}, bpp). \quad (10)$$

(a) Image 1   (b) Image 2   (c) Image 3

(d) Image 4   (e) Image 5   (f) Image 6

(g) Image 7   (h) Image 8   (i) Image 9

(j) Image 10   (k) Image 11   (l) Image 12
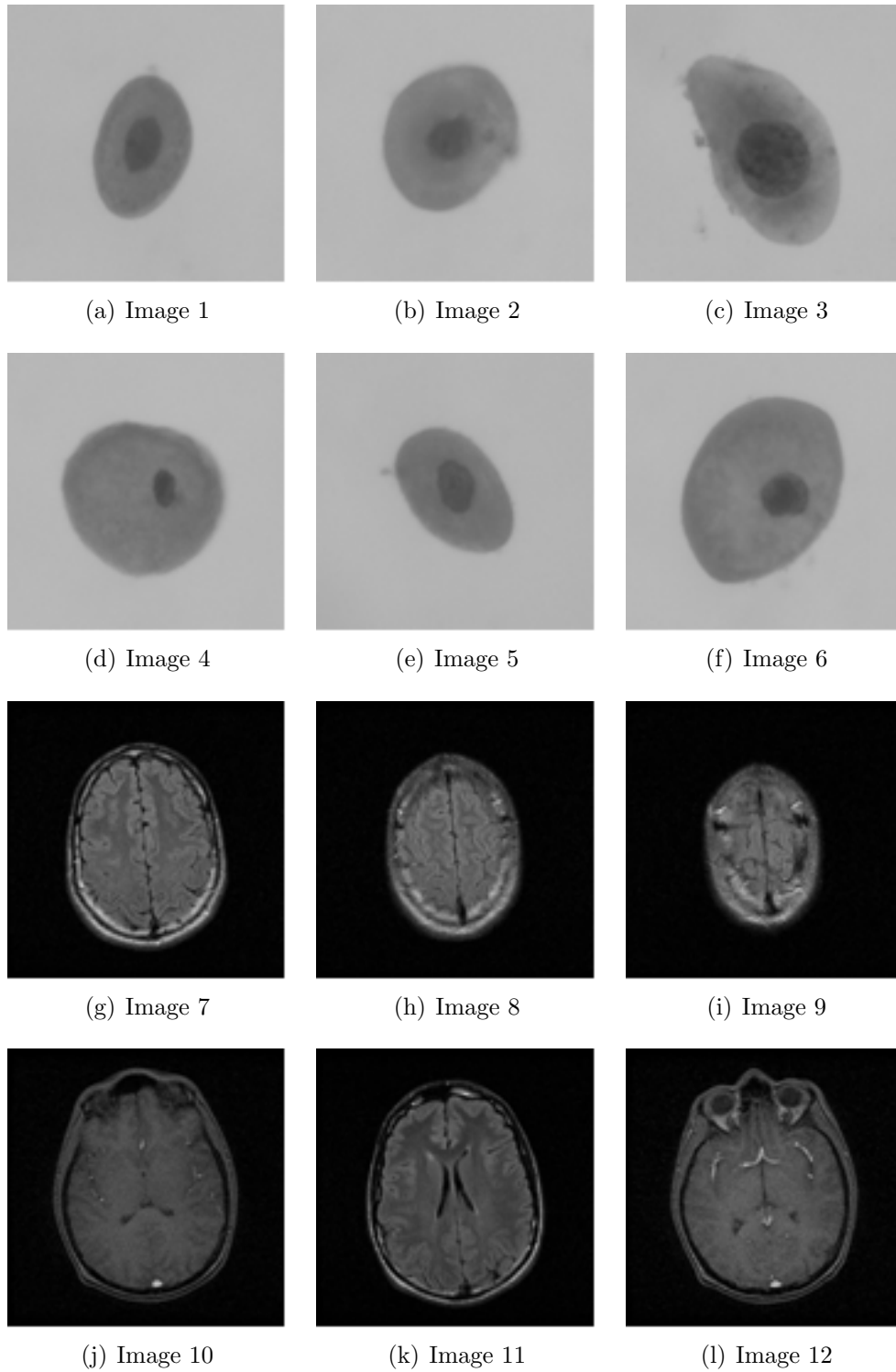
FIGURE 4. Test images

The first experiment is designed to scrutinize the effect of parameter k and k', used in the ROI-based image hiding method, on embedding capacity and the stego-image quality. In this experiment, Images 1, 3, 7 and 11 in Figure 4 were employed to compute the optimal parameters $r_1 = 2.0$, $r_2 = 0.8$ (resp. $r_1 = 2.0$ and $r_2 = 1.7$) by "genetic-based parameter detector" (GBPD) proposed in [8] for segmenting ROIs of the cervical smear images (resp. the brain MRI images). The experimental results are demonstrated

in Table 1, where $|SD|$ is the size of secret data, $|ES|$ the size of extra space, $|ED| = |SD| + |ES|$ the size of embedding data, and R the data embedding rate. Figure 5 demonstrates the stego-images created by the ROI-based image hiding method with $k = k' = 3$. The experimental results tell that the ROI-based image hiding method can provide not only a high data embedding rate but also a high stego-image quality.

The compression ratio plays an important role in deciding the data embedding capacity and the quality of stego-image for the ROI-based image hiding method. A higher compression ratio will increase data embedding capacity since more space can be remained to carry secret data. However, the texture of brain region in the brain MRI image is uneven so that the adaptive arithmetic coding method cannot give a good compression ratio. Therefore, more memory space is required to hold the compression data.

(a) Image 1   (b) Image 2   (c) Image 3   (d) Image 4   (e) Image 5   (f) Image 6

(g) Image 7   (h) Image 8   (i) Image 9   (j) Image 10   (k) Image 11   (l) Image 12
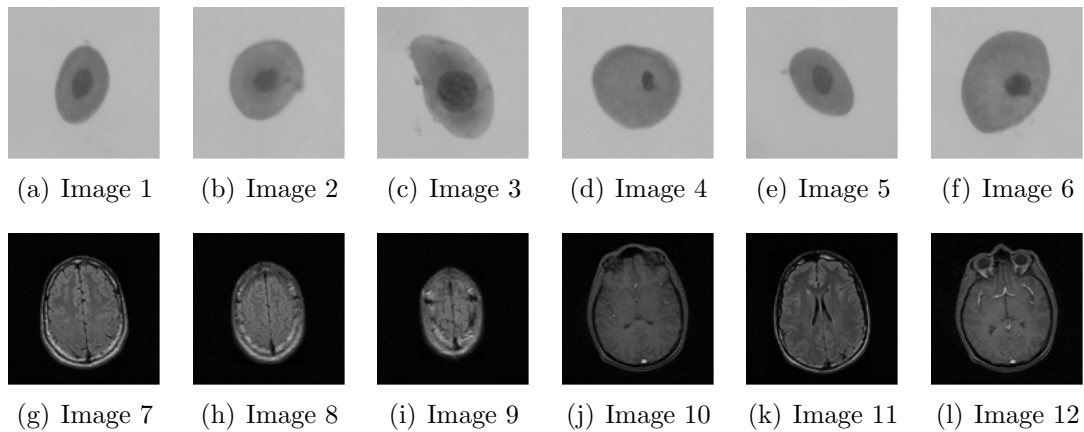
FIGURE 5. Stego-images obtained by ROI-based image hiding method with $k = k' = 3$

(a) ROI-based $(k = k' = 3)$ (b) HPFBRIH $(k' = 3)$ (c) Tian's   (d) SLSB $(k = 3)$ (e) ROI-based $(k = k' = 3)$

(f) HPFBRIH $(k' = 3)$ (g) Ni et al.'s   (h) Tian's   (i) $SLSB$ $(k = 3)$ (j) $SLSB$ $(k = 3)$
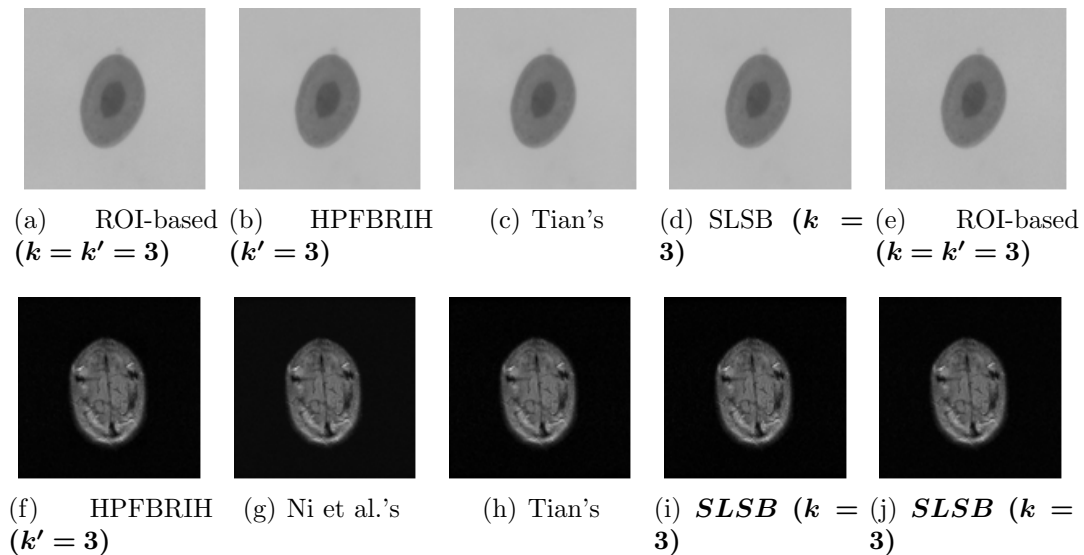
FIGURE 6. The obtained stego-images of images 1 and 9

The second experiment is designed to compare the performance of the ROI-based image hiding method with those of other image hiding methods [1,2,6,9]. Here, the extra data created by these image hiding methods are encoded by the adaptive arithmetic encoding

TABLE 1. Performance of ROI-based image hiding method with different k and k'

Image No.	$k = k' = 2$				
	$PSNR(dB)$	$|ED|(bits)$	$|ES|(bits)$	$|SD|(bits)$	$R(bpp)$
1	47.240	113302	4912	108390	1.654
2	47.668	106014	5616	100398	1.532
3	48.510	93344	9688	83656	1.276
4	48.128	98972	7752	91220	1.392
5	47.416	110662	5184	105478	1.609
6	48.569	93014	8544	84470	1.289
7	47.895	88256	27992	60264	0.920
8	47.184	98908	19960	78948	1.205
9	46.807	105862	15920	89942	1.372
10	48.847	76332	35072	41260	0.630
11	48.809	75632	34480	41152	0.628
12	48.886	75344	45136	30208	0.461
Image No.	$k = k' = 3$				
	$PSNR(dB)$	$|ED|(bits)$	$|ES|(bits)$	$|SD|(bits)$	$R(bpp)$
1	41.621	113302	4912	108390	2.513
2	42.010	106014	5616	100398	2.339
3	42.864	93344	9688	83656	1.979
4	42.477	98972	7752	91220	2.147
5	41.785	110662	5184	105478	2.450
6	41.195	93014	8544	84470	1.995
7	47.895	88256	27992	60264	1.422
8	47.184	98908	19960	78948	1.834
9	46.807	105862	15920	89942	2.077
10	48.847	76332	35072	41260	0.994
11	48.809	75632	34480	41152	0.890
12	48.886	75344	45136	30208	0.461
Image No.	$k = k' = 4$				
	$PSNR(dB)$	$|ED|(bits)$	$|ES|(bits)$	$|SD|(bits)$	$R(bpp)$
1	35.732	226604	5280	221324	3.377
2	36.126	212028	5728	206300	3.149
3	36.938	186688	10320	176368	2.691
4	36.553	197944	7760	190184	2.902
5	35.841	221324	5400	215924	3.295
6	36.948	186028	8752	177276	2.705
7	33.932	176512	44400	132112	2.016
8	33.274	197816	31728	166088	2.534
9	32.829	211724	25840	185884	2.836
10	35.057	152664	56056	96608	1.474
11	34.603	151264	59472	91792	1.401
12	35.179	150688	58504	92184	1.407

TABLE 2. The $k'PSNRs$ and Rs of ROI-based and other image hiding method

Image No.	ROI-based method $(k = k' = 3)$		ROI-based method $(k = k' = 4)$		HPFBRIH method $(k = k' = 3)$		HPFBRIH method $(k = k' = 4)$	
	$PSNR(dB)$	$R(bpp)$	$PSNR(dB)$	$R(bpp)$	$PSNR(dB)$	$R(bpp)$	$PSNR(dB)$	$R(bpp)$
1	41.621	2.513	35.732	3.377	42.209	0.416	35.590	0.666
2	42.010	2.339	36.126	3.149	42.077	0.467	35.479	0.717
3	42.864	1.979	36.938	2.691	42.242	0.405	35.601	0.655
4	42.477	2.147	36.553	2.902	42.109	0.456	35.530	0.706
5	41.785	2.450	35.841	3.295	42.209	0.426	35.611	0.676
6	41.195	1.995	36.948	2.705	42.155	0.461	35.519	0.711
7	40.513	1.422	33.932	2.016	31.838	–	25.415	–
8	40.110	1.834	33.274	2.534	31.344	–	24.980	–
9	42.179	2.077	32.829	2.836	30.966	–	24.65	–
10	41.854	0.994	35.057	1.474	32.621	–	25.953	–
11	42.222	0.890	34.603	1.401	31.937	–	25.651	–
12	41.195	0.959	35.179	1.407	32.890	–	26.032	–
Image No.	Ni et al.'s method		Tian's method		SLSB method $(k = 3)$		SLSB method $(k = 4)$	
	$PSNR(dB)$	$R(bpp)$	$PSNR(dB)$	$R(bpp)$	$PSNR(dB)$	$R(bpp)$	$PSNR(dB)$	$R(bpp)$
1	51.371	0.177	46.144	0.496	37.979	3	33.021	4
2	52.800	0.187	47.332	0.496	37.158	3	33.554	4
3	52.579	0.154	46.029	0.496	37.369	3	32.817	4
4	53.280	0.212	46.864	0.496	36.972	3	33.627	4
5	52.732	0.208	46.873	0.496	38.921	3	32.132	4
6	52.733	0.173	46.132	0.496	37.158	3	33.260	4
7	49.395	0.127	32.963	0.047	37.912	3	31.534	4
8	49.530	0.149	35.822	0.036	37.998	3	31.579	4
9	49.661	0.167	36.820	0.022	38.017	3	31.539	4
10	48.386	0.112	36.241	0.096	37.822	3	31.598	4
11	48.424	0.126	32.281	0.064	37.875	3	31.362	4
12	48.396	0.114	33.957	0.076	37.802	3	31.609	4

method. The compression data are concatenated to the secret data and concealed in the stego-image, too.

Table 2 shows the results of the second experiment. Figure 6 displays the stego-images of Images 1 and 9, produced by the ROI-based method and other compared methods. Since the gray-level intensities of most pixels in brain MRI images are very close to **0** (i.e., the images shown in Figure 2(d)), the gray-level intensities of many pixels in these images will incur underflow after secret data are embedded. Therefore, for a brain MRI image, the compression data of **BM** generated by the adaptive arithmetic encoding method in the HPFBRIH method is too big so that the cover image cannot carry it. The symbol "–" in Table 2 indicates that the cover image cannot hold the whole embedding data.

The experimental results shows that Ni et al.'s method provides a higher image quality than other methods, but it gives far lower **R**. For Tian's method, the obtained average **R** is about **0.5** bpp and most background pixels in a brain MRI image incur underflow. Lou et al.'s [5] method embeds a **1**-bit secret data in the difference between two neighboring pixels. Hence, the maximum data embedding rate is approximate **0.5** bpp. The SLSB method can supply a high data embedding rate than other methods. However, the SLSB method cannot completely recover the cover image only from the stego-image. The ROIs in a medical image have to be protected losslessly. Overall, the ROI-based image hiding method is superior to other methods in data embedding rate and the stego-image quality. In addition, the ROI-based image hiding method can reconstruct the ROIs without any distortion.

6. **Conclusions.** In a medical image, ROIs describe important information that must be restored without any distortion. In this paper, an ROI-based image hiding method has been proposed where ATD is applied to segmenting the ROIs in a medical image. Next, the secret data are hidden in non-ROI by the SLSB method and the remainder of secret data is embedded in ROIs by the HPFBRIH method, so that the ROIs can be completely recovered from the stego-image. The experimental results demonstrate that the ROI-based image hiding method can not only provide a high data embedding rate than other reversible image hiding methods but also a satisfying stego-image image quality.

REFERENCES

[1] C. K. Chan and L. M. Cheng, Hiding data in images by simple LSB substitution, *Pattern Recognition*, vol.37, no.3, pp.469-474, 2004.

[2] C. C. Chang, P. Y. Pai, C. M. Yeh and Y. K. Chan, A high payload frequency-based reversible image hiding method, *Information Sciences*, vol.180, no.11, pp.2286-2298, 2010.

[3] Z. Hou, Q. Hu and W. L. Nowinski, On minimum variance thresholding, *Pattern Recognition Letters*, vol.27, no.14, pp.1732-1743, 2006.

[4] C. F. Lee, C. C. Chang and K. H. Wang, An improvement of EMD embedding method for large payloads by pixel segmentation strategy, *Image and Vision Computing*, vol.26, no.12, pp.1670-1676, 2008.

[5] D. C. Lou, M. C. Hu and J. L. Lin, Multiple layer data hiding scheme for medical images, *Computer Standards & Interfaces*, vol.31, no.2, pp.329-335, 2009.

[6] Z. Ni, Y. Q. Shi, N. Ansari and W. Su, Reversible data hiding, *IEEE Transactions on Circuits and Systems for Video Technology*, vol.16, no.3, pp.354-362, 2006.

[7] N. Otsu, A threshold selection method from gray-level histograms, *IEEE Transactions on Systems, Man, and Cybernetics*, vol.9, no.1, pp.62-66, 1979.

[8] P.-Y. Pai, C.-C. Chang, Y.-K. Chan and M. H. Tsai, An adaptable threshold detector, *Information Sciences*, vol.181, no.8, pp.1463-1483, 2011.

[9] P.-Y. Pai, C.-C. Chang, Y.-K. Chan and C.-C. Liao, Meaningful shadow based multiple gray level visual cryptography without size expansion, *International Journal of Innovative Computing, Information and Control*, vol.7, no.3, pp.1457-1465, 2011.

[10] J. Tian, Reversible data embedding using a difference expansion, *IEEE Transactions on Circuits and Systems for Video Technology*, vol.13, no.8, pp.890-896, 2003.

[11] A. Wakatani, Digital watermaking for ROI medical images by using compresses signature image, *Proc. of the 35th Hawaii International Conference on System Sciences,* vol.6, pp.2043-2048, 2002.